Analysis techniques for the optics in millimetre/submillimetre wave radio telescope receivers

C. Y. Tham[a], G. Yassin[b] and M. Carter[c]
[a]*Faculty of Engineering & Science, Tunku Abdul Rahman University, Malaysia*
[b]*Experimental Astrophysics Group, University of Oxford, U.K.*
[c]*Institut De Radio Astronomie Millimetrique, Saint Martin d'Hères, France*

(Received 25 July 2005)

We present a rigorous analysis technique to design the optics system of millimetre wave radio telescopes. Gaussian optics is used to propagate the beam through the optical system and multimode Gaussian to calculate field distributions. The optical system is modelled as a set of nonlinear equations for the iteration process. A root searching routine is used to find the optimum combination of parameters – mirror focal lengths, relative positions, orientations and sizes. The final antenna performance such as beam efficiency, cross-polarization levels, spillovers are calculated using physical optics. This analysis method was use to design the optics system of the Atacama Large Millimeter Array (ALMA).

I. INTRODUCTION

Designing ground based antennas for millimeter and submillimeter wave astronomy requires rigorous calculation of the electromagnetic fields while the optical elements are many wavelengths across making full wave analysis very time consuming. A novel technique to overcome this difficulty was developed for the ALMA [1] project. ALMA is a state of the art interferometer radio telescope currently being designed and constructed by a large international consortium in northern Chile. The array comprises sixty-four 12-m antennas and is scheduled for first observation in 2010. The telescope focal plane receivers cover ten frequency bands corresponding to the atmospheric windows between 10 mm and 350 μm. The array beselines can be configured from 150 m to 10 km producing spatial resolution of 10 milliarcseconds. ALMA will also have detectors of unprecedented sensitivity and it is expected to have huge impact on many areas of astrophysics such as star formation and cosmology.

A typical optics arrangement for ALMA antenna is shown in Fig. 1. The system consists of a pair of corrugated feed horns (one for each orthogonal polarization), two ellipsoid mirrors, the hyperboloid subreflector and the paraboloid main reflector. The off axis feed system allows the receivers of all the ten frequency bands to view the sky simultaneously. A modular receiver design was adopted to minimise the effort required for assembly and maintenance at the hostile site condition. The feed optics for each band comprising the feed horns, the mixer, the ellipsoidal mirrors and the driving electronics are fitted into a compact self contained cartridge in the cryostat.

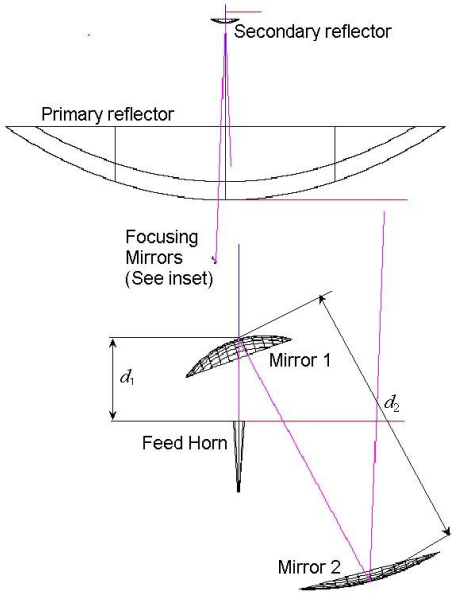

FIG. 1. Optical system of a Cassegrain antenna comprising the primary and secondary reflectors and the feed optics.

The initial design was made using Gaussian beam quasioptics to arrive at the basic system configuration and defining physical parameters [2]. The two ellipsoid mirrors propagate the field from the horn aperture and focus the beam at the Cassegrain focus. The mirror parameters, their orientations, sizes, focal lengths or radii of curvature and positions are critical to the performance. The orientations or angles of incidence of the off-axis mirrors are designed for minimum distortion and cross-polarization and maximum antenna efficiency. Varying these parameters not only changes the overall optical performance but may also breach the physical constraint. Changes in the beam radius along the optical path affect the truncation losses at the mirrors and

apertures. Moreover, the optimised optical system must fit into the physical confine of the compact cartridge in the cryostat. Finally optimum system performance must be maintained across a large bandwidth. Following optimisation, the antenna performance indicators are calculated using physical optics. The key indicators of the antenna performance include the circularity of the field incident on the subreflector, spillover and noise contributed by each reflector, the antenna far field pattern, beam efficiency and cross-polarization levels.

II. ANALYSIS METHOD

Consider a distant source in the sky illuminating the aperture of an antenna with a plane wave field. This field is to be coupled with maximum efficiency to the Gaussian field from the corrugated feed horn after going through scattering and distortion by the off-axis optical system. The level at which this Gaussian field is truncated at the subreflector determines the coupling efficiency. The diameter of the subreflector is designed for minimum blockage. Small diameter means high truncation of the Gaussian field producing high taper efficiency but increases spillover and thus reduces the aperture efficiency. Obviously the symmetry of the distorted Gaussian field will affect the efficiency.

The power distribution across the profile of a Gaussian beam may be written as:

$$\frac{P(r_e)}{P(0)} = \exp\left(\frac{-2r^2}{w^2}\right), \tag{1}$$

where r is the distance from the beam axis, and w is the beam waist. The aperture efficiency of a Cassegrain antenna is a function of the edge taper as well as the fractional blockage due to the subreflector. The edge taper is defined as the relative power density at a radius $r = r_e$,

$$T_e = -10\log_{10}\left(\frac{P(r_e)}{P(0)}\right), \tag{2}$$

and the fractional blockage is the ratio of the subreflector radius to that of the main reflector, $f_b = r_s / r_a$. Optimum aperture efficiency is achieved by balancing the taper efficiency against the spillover efficiency. The aperture efficiency is given by [3]

$$\varepsilon_a = \varepsilon_t \cdot \varepsilon_s, \tag{3}$$

where ε_t is the taper efficiency and ε_s is the spillover efficiency given respectively by

$$\varepsilon_t = \frac{\left|\iint_a E_a dS\right|^2}{\left|\iint_a |E_a|^2 dS \cdot \iint_a dS\right|} \tag{4}$$

and

$$\varepsilon_s = \frac{\iint_a |E_a|^2 dS}{\iint_{ap} |E_a|^2 dS}. \tag{5}$$

E_a is the field over the aperture plane, *a* denotes area over the aperture and *ap* that over the entire plane at the aperture.

For the ALMA antenna r_s = 375 mm and r_a = 6000 mm the optimum aperture efficiency is 80.34% which is obtained for an edge taper = 10.81 dB as shown in Fig. 2. The figure also shows that at the maximum, the aperture efficiency is relatively insensitive to the variation of the edge taper within at least ± 1 dB. The efficiency falls to 80.06% at T_e = 9.81 dB and 80.10% at T_e = 11.81 dB. The field from a corrugated feed horn may be approximated more closely by the Bessel function $J_0(r)$ which has a higher optimum efficiency of 85.52% at T_e = 9.93 dB. An optimization procedure that is accurate to this level of tolerance will be effective.

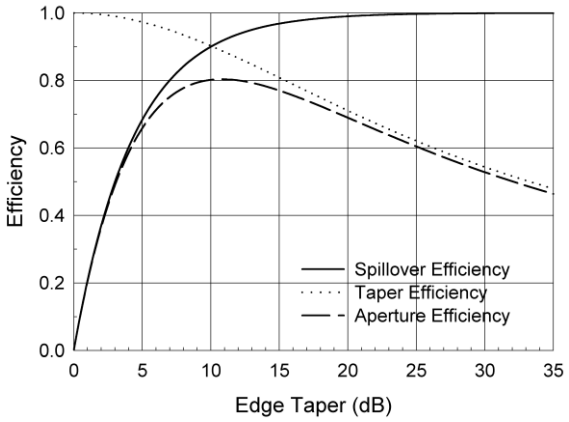

FIG. 2. Aperture efficiency for a Cassegrain antenna with fractional blockage f_b = 375/6000 as a function of edge taper.

In Fig. 1, the distances crucial to achieving optimum performance are labelled as, d_1 from the horn aperture to the centre of the first mirror, d_2 between the first and second mirror and, d_3 from the second mirror to the Cassegrain focus. The second mirror is positioned with respect to the Cassegrain focus so that the focus is kept close to the cryostat window. A small beam radius at the window allows the use of a small aperture size to keep down infrared loading on the cryogenics. The value of d_3

together with that of the optimum edge taper are therefore two fixed parameters for the optical system.

The aim now is to find the combination of d_1, d_2, and the corresponding mirror focal lengths f_1 and f_2 that together will yield the target values of d_3 and the edge taper T_e. Moreover the optimisation parameters must produce the desired values of d_3 and T_e across the whole frequency band.

Fundamental Gaussian beam quasioptics is based on the solution of the paraxial wave equation with a scalar field given by

$$E(r,z) = \sqrt{\frac{2}{\pi w^2}} \exp\left(\frac{-r^2}{w^2} - jkz - \frac{j\pi r^2}{\lambda R} + j\phi_0 \right), \tag{6}$$

where

$$R = z + \frac{1}{z}\left(\frac{\pi w_0^2}{\lambda} \right)^2, \tag{7}$$

$$w = w_0 \sqrt{\left[1 + \left(\frac{\lambda z}{\pi w_0^2} \right)^2 \right]} \tag{8}$$

and

$$\tan\phi_0 = \frac{\lambda z}{\pi w_0^2}. \tag{9}$$

The radius of curvature R, beam radius w and phase ϕ_0 completely characterise the beam at each location z along its propagation path. The beam is propagated and transformed by an optical component using the ABCD matrix representing the transforming property of the element [3]. The free propagation and the thin lens matrices are given respectively by

$$\mathbf{M}_{distance} = \begin{bmatrix} 1 & L \\ 0 & 1 \end{bmatrix} \quad \text{and} \quad \mathbf{M}_{lens} = \begin{bmatrix} 1 & 0 \\ -1/f & 1 \end{bmatrix} \tag{10}$$

where L is the propagation distance and f is the focal length of the lens. The complex beam parameter q, which is related to the radius of curvature R and beam radius w by

$$R = \frac{1}{\mathrm{Re}(1/q)} \tag{11}$$

and

$$w = \sqrt{\frac{\lambda}{\pi\,\mathrm{Im}(-1/q)}}, \tag{12}$$

is transformed by

$$q_2 = \frac{Aq_1 + B}{Cq_1 + D} \tag{13}$$

where A, B, C, D are elements of the matrix and the subscripts 1 and 2 refers to the input and output at the component respectively.

The beam parameters R, w and ϕ_0 are first calculated at the aperture of the feed horn. For a corrugated horn the optimum beam radius that couples to the fundamental Gaussian mode $w = 0.644a$ where a is the aperture radius. The beam is propagated using thin lenses to approximate the ellipsoid mirrors. For any combination of d_1, d_2, f_1 and f_2, the focal point d_3, is found to any specified precision using an iterative algorithm.

When the antenna is in focus the radius of curvature of the beam equals that of the subreflector giving a flat phase front. In this case the search is for this position z_{SR} along the propagation path. For the ALMA antenna, the subreflector has a radius of curvature = 6000 mm. The value of the Gaussian beam radius w at this position gives the edge taper T_e from Eq. (1) and Eq. (2).

The fundamental Gaussian field given in Eq. (6) above is a first order solution of the paraxial wave equation. The general solution includes higher order modes and may be expanded in terms of Gauss-Laguerre Polynomials as:

$$E_{pm}(r,\varphi,z) = \sqrt{\left[\frac{2p!}{\pi(p+m)!} \right]} \frac{1}{w(z)} \left[\frac{\sqrt{2}r}{w(z)} \right]^m L_{pm}\left(\frac{2r^2}{w^2(z)} \right) \cdot \exp\left[\frac{-r^2}{w^2(z)} - jkz - \frac{j\pi r^2}{\lambda R(z)} - j(2p+m+1)\phi_0(z) \right] \cdot \exp(jm\varphi), \tag{14}$$

where L_{pm} is the generalised Laguerre polynomials, p is the radial index and m the angular index, φ is the polar angle. The modal expansion method propagates the field solution both in the near and the far field. This is use to calculate the edge taper and other parameters of the system. Other methods are used to estimate the distortion and cross-polar scattering caused by the off-axis mirrors [4,5]. Results in Fig. 2 illustrate that multimode method is sufficiently accurate for our optimization technique.

The optimization process is implemented by casting the optical system as a nonlinear function. Within the constrained range, d_1 and d_2 are varied in regular increment at steps from the lowest allowed value. The stepping is run in a two level loop; for each value of d_1, d_2 runs through the range. For each set of (d_1, d_2) f_1 and f_2 are used as the two input variables in a root finding algorithm. A NAG routine using a modification of the Powell hybrid method is used [6,7]. Initial guess values for f_1 and f_2 are entered to start the search. The calculation returns the values of d_3 and T_e. The

deviations Δd_3 and ΔT_e from the target values, d_3' and T_e' are the residues of the optimization function, where

$$\Delta d_3 = d_3 - d_3' \tag{15}$$

and

$$\Delta T_e = T_e - T_e' . \tag{16}$$

The values of f_1 and f_2 that achieve convergence in d_3 and T_e for each d_1 and d_2 pair are calculated first for the mid-band frequency. The corresponding sets of f_1^l, f_2^l and f_1^h, f_2^h are also calculated for the low and high band edge frequencies respectively. The deviations of the focal lengths from the mid-band values

$$\Delta f_i^p = f_i^p - f_i , \tag{17}$$

where i = 1, 2 and $p = l, h$ are plotted against d_2 for each d_1. The plots reveal that the two Δf lines of each mirror cross at some point close to zero. At this point (d_1, d_2) the mirror with the calculated value of f_i is closest to frequency independence. However the point at which one mirror is frequency independent is normally not for the other. Any combination with all the four Δf deviations from the mid-band value falling within the precision for manufacturing tolerance of the mirrors (5-10 μm) will suffice. There is more than one value of d_1 that this condition can possibly be satisfied. The final selection for the combination of d_1 and d_2 may be based on other performance or practical considerations such as space constraint or manufacturing considerations.

III. RESULTS

Fig. 3 shows the field from the feed horn of the ALMA Band 6 optics at the plane d_1 = 46 mm corresponding to the position of the first mirror. The field calculated using multimode Gaussian is compared against that calculated using a physical optics software [8]. The physical optics result is calculated using an ideal corrugated horn designed to operate with the HE11 hybrid mode field. Fig. 4 shows the field at the plane of the Cassegrain focus located at d_3 = 230 mm from mirror 2. The fields shown in both Fig. 3 and Fig. 4 are for the band 6 mid-frequency of 243 GHz.

Fig. 5 shows the beam profile at the plane of the subreflector at the band 6 mid-band frequency (243 GHz). Results calculated using both multimode Gaussian and physical optics are shown. Fig. 6 shows the far field radiation pattern of the antenna obtained using a corrugated feed horn. To model this the far field horn pattern is first obtained using mode matching [9]. The horn pattern is then used to calculate the incident field on the first mirror using spherical wave expansion technique. The offset optics produces a corresponding offset far field beam axis.

IV. CONCLUSION

A fast and sufficiently accurate optimization procedure for multi reflector millimeter wave optical systems is presented. The results show the proposed procedure is effective in arriving at the optimum combination of the design parameters and frequency independent design can be achieved to the level of acceptable tolerance.

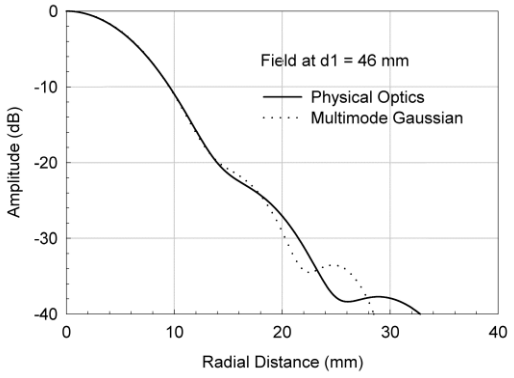

FIG. 3. Field of ideal corrugated horn at d_1 = 46 mm from its aperture, frequency 243 GHz.

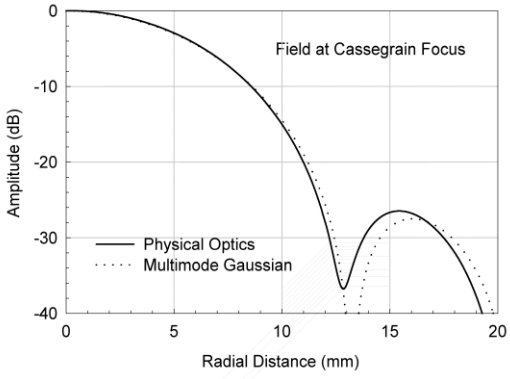

FIG. 4. Field at Cassegrain focus plane, d_3 = 230 mm from mirror 2, frequency 243 GHz.

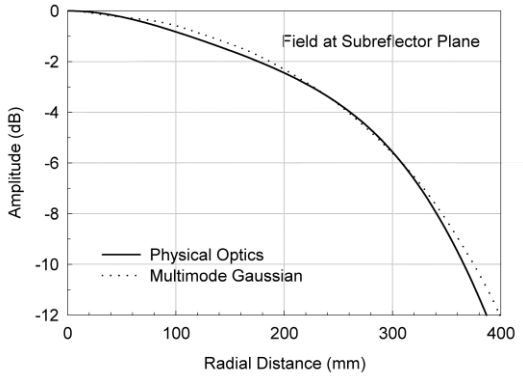

FIG. 5. Beam profile at the subreflector at mid-band frequency (243 GHz).

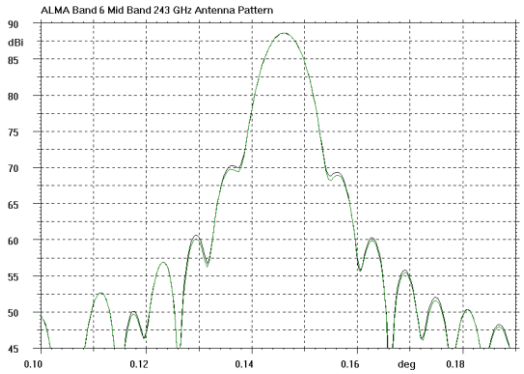

FIG. 6. Antenna radiation pattern on antenna axis coordinates showing the offset of the beam.

REFERENCES

[1] Website http://www.alma.nrao.edu/

[2] J. W. Lamb, A. Baryshev, M. C. Carter, L. R. D'Addario, B. N. Ellison, W. Grammer, B. Lazareff, Y. Sekimoto, and C. Y. Tham, "ALMA Receiver Optics Design", ALMA Memo, **362**, The Atacama Large Millimetre Array Project, National Radio Astronomy Observatory, Tucson, AZ, Apr. 11 (2001).

[3] Paul F. Goldsmith, *Quasioptical Systems; Gaussian Beam, Quasioptical Propagation and Applications*, IEEE Press, New York, N.Y. (1998).

[4] J. A. Murphy, "Distortion of a simple Gaussian beam on reflection from off-axis ellipsoidal mirrors," Int. J. of Infrared and Millimeter Waves, **8(9)**, 1165-1187 (1987).

[5] C. Dragone, "Offset multireflector antennas with perfect pattern symmetry and polarization discrimination," The Bell System Tech. Jour., **57(7)**, 2663-2684 (1978).

[6] *The NAG FORTRAN Library Manual Mark 19*, The Numerical Algorithms Group Ltd., Oxford, U.K., and The Numerical Algorithm Group, Inc., Downers Grove, IL. (1999).

[7] M. J. D. Powell, "A hybrid method for nonlinear algebraic equations in numerical methods for nonlinear algebraic equations, ed. P. Rabinowitz , Gordon and Breach (1970).

[8] GRASP8 version 8.2.5, TICRA Engineering Consultants, Copenhagen, Denmark (2002).

[9] A. D. Olver, P. J. B. Clarricoats, A. A. Kishk, and L. Shafai, *Microwave Horns and Feeds*, IEEE Press, IEE, London and IEEE, Inc., New York (1994).